Nucleic Acids Research, 2001, Vol. 29, No. 13 2757–2765

Initiation of HIV-2 reverse transcription: a secondary structure model of the RNA–tRNA^{Lys3} duplex

Frédéric Freund, Florence Boulmé, Simon Litvak and Laura Tarrago-Litvak*

UMR-5097, CNRS-Université Victor Segalen Bordeaux 2, Case 103, 146 rue Léo Saignat, 33076 Bordeaux cedex, France. IFR 66 'Pathologies Infectieuses', Bordeaux

Received March 15, 2001; Revised and Accepted May 15, 2001

ABSTRACT

Human immunodeficiency virus type 2 (HIV-2) reverse transcription is initiated from cellular tRNA^{Lys3} partially annealed to the RNA viral genome at the primer binding site (PBS). This annealing involves interactions between two highly structured RNA molecules. In contrast to HIV-1, in which the reverse transcription initiation complex has been thoroughly studied, there is still little information regarding a possible model to describe the secondary structure of the template–primer complex in HIV-2. To determine whether HIV-2 RNA sequences flanking the PBS may specifically interact with the natural primer tRNA, we performed site-directed mutagenesis and enzymatic footprinting. An RNA fragment corresponding to the HIV-2 U5 RNA domain and tRNA^{Lys3} were probed either in their free form or in the binary complex. Important reactivity changes to nucleases were obtained upon complex formation. In addition to the canonical contacts between the viral PBS and the 3′ end acceptor stem of tRNA^{Lys3}, we identified two additional interacting domains: (i) the U-rich region of the anticodon loop with the A-rich sequence of the internal loop within the U5-prePBS region; (ii) nucleotides 48–54 from the TΨC domain of tRNA^{Lys3} and the 240–247 region of viral U5-RNA. In view of these experimental data and sequence comparison between different HIV-2 isolates, we propose a model for the secondary structure of the HIV-2 template–primer initiation complex.

INTRODUCTION

Reverse transcription of a retroviral genome involves the conversion of the single-stranded genomic RNA into a double-stranded DNA molecule catalysed by the viral reverse transcriptase (RT) (reviewed in 1). This enzyme initiates *in vivo* cDNA synthesis from the terminal 3′-OH group of a host tRNA (reviewed in 2). The primer for human immunodeficiency virus type 1 and type 2 (HIV-1 and HIV-2) is tRNA^{Lys3}. In all retroviruses the 3′ end of the tRNA is annealed to the primer binding site (PBS), a complementary region of 18 nt located near the 5′ end of the viral genome.

The initiation of reverse transcription requires specific interactions within two highly structured nucleic acids, the viral RNA genome and primer tRNA. Besides the main interaction between the PBS and the 3′ end of tRNA, additional interactions have been identified. In HIV-1, the interaction between the A-rich loop from the U5 region upstream of the PBS and the U-rich anticodon loop of tRNA has been implicated in the initiation of cDNA synthesis (3–6), as well as in the positioning of tRNA^{Lys3} on the PBS (7). The importance of this interaction has also been shown in HIV-1 infected cells in which HIV-1 RNA containing a deletion of the A-rich loop showed decreased reverse transcription (8). Moreover, an HIV-1 RNA, whose PBS region was mutated to be complementary to the 3′ ends of tRNA^{Met} or tRNA^{His}, was not conserved in infected cell culture (9–12). However, when the A-rich loop was altered to anneal to the anticodon loop of the corresponding tRNA primers, the mutated PBS sequence was maintained upon long-term cell culture.

The replication of HIV-2 has not been investigated as extensively as that of HIV-1. In contrast to HIV-1, in which the structural and functional features of the reverse transcription initiation complex have been thoroughly studied, the structure of the HIV-2 template–primer complex is much less well known. A model of the secondary structure of the genomic RNA leader region of the HIV-2$_{ROD}$ isolate has been reported (13). This structure was predicted on the basis of chemical and enzymatic footprints, computer analysis and phylogenetic comparisons of sequences from different HIV-2 isolates (Fig. 1). The secondary structure proposed for the U5 region from HIV-2$_{ROD}$ is more complex than that of HIV-1. While HIV-1 has only one A-rich single-stranded region in the stem–loop 5′ upstream of the PBS, HIV-2 RNA has two A-rich regions. On the other hand, the HIV-2 prePBS stem–loop structure corresponding to nucleotides 244–305 is very stable with a ΔG of –120 kJ, calculated with Zuker's program (14), compared to –38 and –17 kJ for the same structures in HIV-1 (MAL and LAI, respectively).

In the absence of crystal structures or crosslinking studies on the HIV-2 RNA–tRNA^{Lys3} template–primer complex, the use

*To whom correspondence should be addressed. Tel: +33 5 57 57 17 60; Fax: +33 5 57 57 17 66; Email: laura.litvak@reger.u-bordeaux2.fr
Present addresses:
Frédéric Freund, Département de Microbiologie et d'Immunologie, Université de Montréal, Montréal, Québec H3C 3J7, Canada
Florence Boulmé, Institute of Medical Biochemistry, Department of Molecular Biology, Vienna Biocenter. Dr Bohrgasse 9, 1030 Vienna, Austria

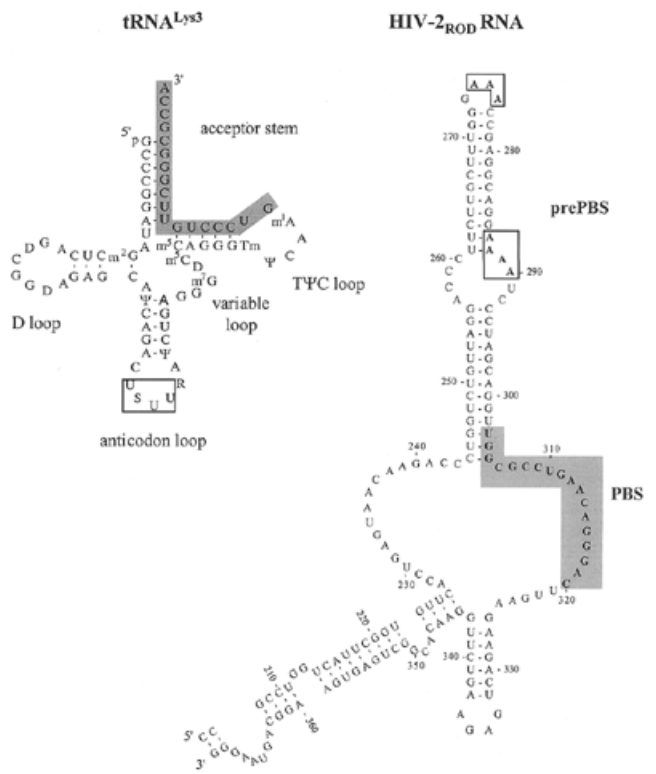

Figure 1. Secondary structures of $tRNA^{Lys3}$ and the HIV-2_{ROD} U5-PBS region [adapted from Berkhout and Schoneveld (13)]. Dark boxes, principal interaction of the reverse transcription initiation complex between the viral PBS region and the primer acceptor stem. White boxes, the primer anticodon loop may interact with one of the two A-rich viral RNA regions.

of alternative strategies may be useful to demonstrate the existence of loop–loop interactions and to characterise their role in the initiation of reverse transcription. Using an antisense approach we have recently shown that the HIV-2 A-rich internal loop ($_{287}AAAA_{290}$) is able to interact with the U-rich anticodon of the $tRNA^{Lys3}$ primer (15).

In the present study we combined site-directed mutagenesis and enzymatic probing of both partners engaged in the template–primer initiation complex to obtain further information about the structural rearrangements taking place upon complex formation. The results showed other secondary structure elements in interaction, besides those concerning the acceptor stem of $tRNA^{Lys3}$ and the PBS involved in the *stricto sensu* priming. These new interactions were formed between the A-rich internal prePBS loop and the U-rich anticodon, as well as between a region of HIV-2 U5 and the stem of the TΨC stem–loop from $tRNA^{Lys3}$. All these data taken together with sequence comparison between different HIV-2 isolates has allowed us to establish a secondary structure model of the HIV-2 $tRNA^{Lys3}$–viral RNA primer–template initiation complex.

MATERIALS AND METHODS

Proteins

HIV-2 RT RNase H^- was expressed in transformed *Escherichia coli* (15) and purified as previously described (16). T7 RNA polymerase was from Stratagene; DNase I, *Nco*I and mung bean nuclease (MBN) from Gibco BRL Life Technologies Inc.; human placental RNase inhibitor (RNasin) from Promega; bacteriophage T4 polynucleotide kinase from New England Biolabs Inc.; ribonuclease V1 and RNA ligase from Pharmacia.

Mutagenesis

The QuickChange™ Site-Directed Mutagenesis Kit was from Stratagene.

Nucleotides

Radioisotopes [α-^{32}P]dATP (3000 Ci/mmol), [α-^{32}P]dCTP (3000 Ci/mmol), [γ-^{32}P]ATP (3000 Ci/mmol) and [α-^{32}P]pCp (3000 Ci/mmol) were purchased from Amersham Laboratories. Unlabelled nucleotides [deoxyribonucleoside triphosphates (dNTPs) and ribonucleoside triphosphates (rNTPs)] were from Gibco BRL Life Technologies Inc.

Oligodeoxynucleotides (ODNs)

The nucleotide sequence of the HIV-2_{ROD} strain (13) was used to design all the antisense ODNs. ODNs 303–320 and 372–390 were purchased from MGW-Biotech AG.

$tRNA^{Lys3}$

Beef liver $tRNA^{Lys3}$ was purified as previously described (16).

In vitro HIV-2 RNA synthesis

The HIV-2_{ROD} RNA fragment containing nucleotides 1–545 (a kind gift from Dr J.-L. Darlix, INSERM U-412, Lyon, France) was sub-cloned in a pBluescript vector. *Escherichia coli* XL-1 Blue was used for plasmid amplification. After digestion of the HIV-2_{ROD} clone with *Nco*I (position 545) and *in vitro* transcription using the T7 RNA polymerase, we obtained RNA starting at position +1. Three micrograms of linearised plasmid DNA were transcribed in a reaction mixture (final volume 0.1 ml) containing 40 mM Tris–HCl (pH 8.0), 8 mM $MgCl_2$, 10 mM spermidine, 25 mM NaCl, 10 mM dithiothreitol (DTT), 0.5 mM of each rNTP, 100 U of T7 RNA polymerase and 20 U of RNasin, for 1.5 h at 37°C. After treatment with 12 U of RNase-free DNase I for 10 min at 37°C, RNA transcripts were extracted with 1 vol of phenol/chloroform/isoamyl alcohol (24/24/1) and 1 vol chloroform, and precipitated by addition of 2.5 vol of ethanol and 0.3 M ammonium acetate.

Reverse transcription with an HIV-2 RNA template

As described before (17), reverse transcription was performed in a total volume of 10 µl containing 50 mM Tris–HCl pH 8.0, 6 mM $MgCl_2$, 2 mM DTT, 10 mM NaCl, 100 nM HIV RNA, 0.3 mM of each dNTP, 1 µM of synthetic ODN primer complementary to HIV-2 RNA and 5 µCi [α-^{32}P]dCTP (3000 Ci/mmol). Template and ODN primer were incubated for 15 min at 37°C. Then, the dNTP mixture, [α-^{32}P]dCTP, 150 nM RT (RNase H^-) and 0.2 U RNasin were added. Incubation was carried out for 45 min at 37°C and the reaction was stopped by adding 3 µl of electrophoresis loading buffer (95% formamide, 0.5 mM EDTA, 0.025% bromophenol blue, 0.025% xylenecyanol, 0.025% SDS). The reaction products were analysed by electrophoresis on 6% polyacrylamide–TBE–7 M urea denaturing gels. After the run, gels were autoradiographed and films scanned using the NIH Image Program (Macintosh).

Directed mutagenesis of HIV-2 RNA

The QuickChange™ Site-Directed Mutagenesis Kit (Stratagene) was used. A mutated HIV-2_{ROD} RNA (nucleotides 1–545) containing $_{274}CUU_{276}$ [called $mut_{(274–276)}$ RNA] instead of the wild-type $_{274}AAA_{276}$ fragment, or $_{287}AGUU_{290}$ [called $mut_{(287–290)}$ RNA] instead of the wild-type $_{287}AAAA_{290}$ fragment was obtained by transcription of the mutated plasmid.

$tRNA^{Lys3}$ labelling

3′ End labelling. The $tRNA^{Lys3}$ (1 µg) was labelled at its 3′ end with 100 µCi of [α-^{32}P]pCp (3000 Ci/mmol) in ligation buffer (50 mM HEPES pH 7.5, 15 mM $MgCl_2$ and 3.3 mM DTT), in the presence of 1 mM ATP, 0.1 mg/ml of bovine serum albumin and 1300 U/ml T4 RNA ligase in 30 µl final volume. The reaction was incubated overnight at 4°C and stopped with 10 µl of loading buffer. The labelled [α-^{32}P]pCptRNA^{Lys3} was purified by electrophoresis on 8% denaturing polyacrylamide gel.

5′ End labelling. The $tRNA^{Lys3}$ (1 µg) was mixed with 100 µCi of [γ-^{32}P]ATP (3000 Ci/mmol) in the exchange buffer (50 mM imidazole–HCl pH 6.4, 12 mM $MgCl_2$, 1 mM 2-mercaptoethanol, 70 µM ADP), in the presence of 5 U T4 polynucleotide kinase in a final volume of 25 µl. The reaction was performed for 1 h at 37°C, stopped with 10 µl of loading buffer and the labelled [^{32}P]$tRNA^{Lys3}$ was extracted as described above.

Enzymatic probing of $tRNA^{Lys3}$

Either 5′ end labelled ^{32}P-$tRNA^{Lys3}$ or 3′ end [α-^{32}P]pCptRNA^{Lys3} (0.1 pmol) was hybridised to the RNA_{ROD} fragment (1 pmol) by heating at 95°C for 2 min, followed by slow cooling. The enzymatic digestion of the ^{32}P-$tRNA^{Lys3}$–viral RNA complex by MBN was performed in 30 µl at 37°C for 7 min, in the presence of 10 mM sodium acetate pH 5.0, 0.01 mM zinc acetate, 0.1 mM L-cysteine, 3 mM NaCl, 6 mM $MgCl_2$ and different concentrations of MBN. Nuclease digestion of the [α-^{32}P]pCptRNA^{Lys3}–viral RNA complex was performed in 30 µl at 37°C for 7 min, in the presence of 20 mM Tris–HCl pH 7.2, 200 mM NaCl, 6 mM $MgCl_2$ and different concentrations of ribonuclease V1. The reaction was stopped with 1 vol of phenol/chloroform/isoamyl alcohol (24/24/1 v/v/v) and 3 µl of loading buffer were added to the aqueous phase previously recovered. Samples were analysed on 15% denaturing polyacrylamide gel.

Enzymatic probing of viral RNA

After prehybridising $tRNA^{Lys3}$ (5 pmol) to the RNA_{ROD} fragment (0.5 pmol), the complex was digested in the same conditions as described above. The reaction products were extracted with 1 vol of phenol/chloroform/isoamyl alcohol and RNAs were precipitated with ethanol. RNA cleavage sites were identified by the reverse transcription reaction as follows: the digestion products were preincubated for 15 min at 37°C with two different primers, either an anti-PBS ODN (nucleotides 303–320) or an ODN primer (nucleotides 372–390), and then incubated for 5 min in the presence of 5 µCi [α-^{32}P]dNTP, 150 nM RT and 0.2 U human placental RNase inhibitor (the labelled dNTP was dATP for the anti-PBS primer and dCTP for the other ODN primer). The incubation was performed for 45 min at 37°C in the presence of the four dNTPs, and the reaction was stopped by the addition of 3 µl loading buffer. Samples were analysed by electrophoresis on a 15% denaturing polyacrylamide gel.

RESULTS AND DISCUSSION

Our aim in this work was to obtain further information about the replication of HIV-2 and more specifically on the initiation of the reverse transcription step, a crucial target of antiviral agents. To analyse the structural changes occurring upon formation of the HIV-2 primer–template reverse transcription initiation complex, we probed $tRNA^{Lys3}$ and the U5 HIV-2_{ROD} RNA fragment, both in the free state and the binary complex. Digestion patterns were obtained by using structure-specific nucleases, the MBN, a specific nuclease of single-stranded nucleic acids and ribonuclease V1, a specific enzyme of double-stranded structures.

Probing of $tRNA^{Lys3}$

Labelled $tRNA^{Lys3}$, either free or hybridised to HIV-2_{ROD} RNA (nucleotides 1–545), was subjected to limited digestion with RNase V1 and MBN. The positions of enzymatic cleavages within tRNA were identified by the size of the radioactive fragments. Figure 2A shows the cleavage products obtained when $tRNA^{Lys3}$ alone (lanes 2–5) or annealed to the viral RNA (lanes 6–9) was digested with increasing amounts of ribonuclease V1. Figure 2B corresponds to the MBN digestion pattern of $tRNA^{Lys3}$ alone or annealed to viral RNA (lanes 2–5 and 6–9, respectively). To compare the intensities of the cleavage bands obtained with either free or complexed tRNA, the concentration of RNA substrate was kept constant by adding an RNA which was non-complementary to the primer $tRNA^{Lys3}$ (a 528 nt RNA fragment coding for the retroviral REV protein). Data obtained with both nucleases are summarised in Figure 2C.

When free $tRNA^{Lys3}$ was probed with ribonuclease V1, strong cleavage bands (that became stronger with increasing enzyme concentrations) were observed at sites corresponding to the region C_{28}–A_{31}, as well as a weaker cleavage at nucleotide U_{41} (Fig. 2A, lanes 2–5). These nucleotides are present in the stem of the anticodon stem–loop. The treatment of free tRNA with MBN (Fig. 2B, lanes 2–5) produced single-stranded cleavages on the D-loop, the variable loop and the anticodon loop (Fig. 2C). The V1 and MBN digestion profiles were in agreement with the general cloverleaf structure of a native tRNA.

A striking result was obtained when $tRNA^{Lys3}$ was probed with the nucleases after formation of the binary complex with vRNA. In this case, extremely important changes in reactivity were observed. As shown in Figure 2A (lanes 6–9) the annealed tRNA became more accessible to ribonuclease V1. The most dramatic changes between free and complexed tRNA were observed at positions 48–52 of the stem of the TΨC stem–loop. Strong bands appeared after ribonuclease V1 treatment. These corresponded to cleavage sites at m^5C_{49} and A_{50}. Less intensive bands corresponding to nucleotides m^5C_{48}, G_{51} and G_{52} were also present.

Other changes observed after complex formation concerned the cleavage bands corresponding to the C_{28}–A_{31} region. These bands became more intense (Fig. 2, compare lane 3 with

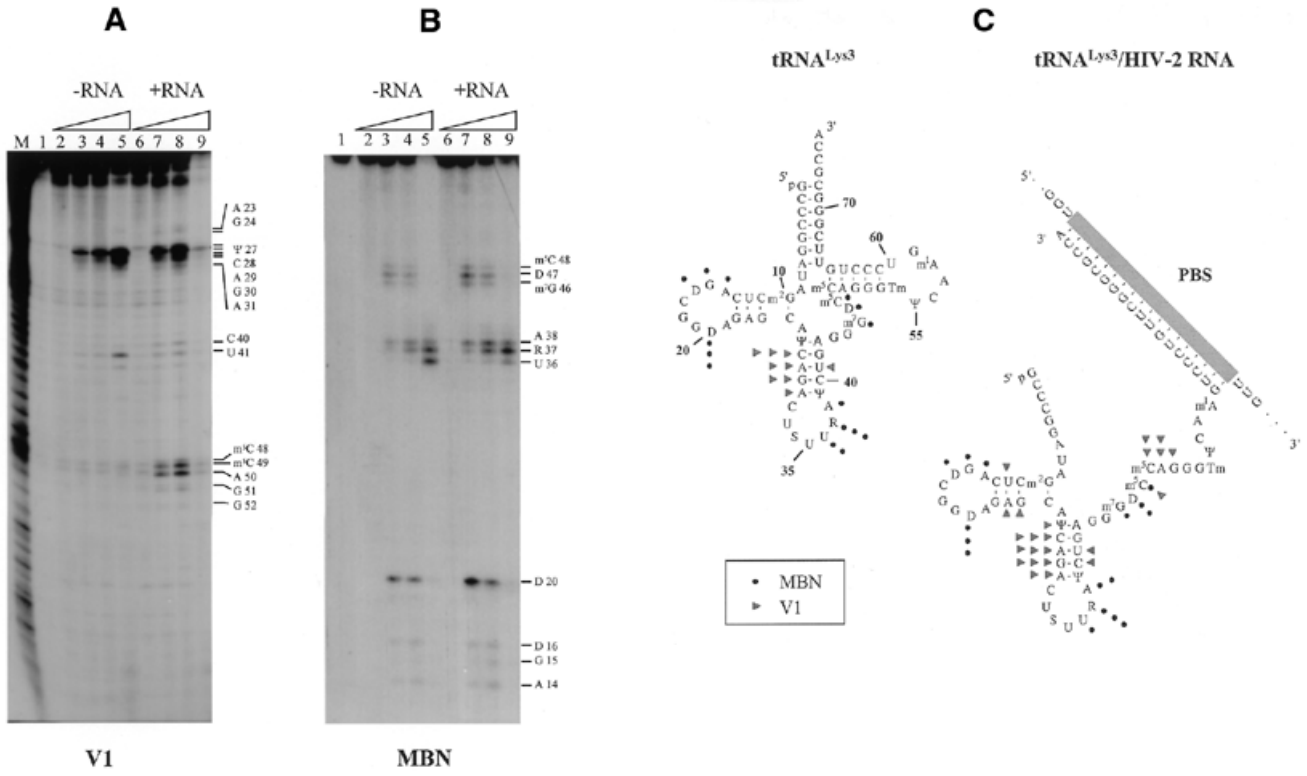

Figure 2. Digestion patterns of free $tRNA^{Lys3}$ or in the binary complex with HIV-2_{ROD} viral RNA. (**A**) Enzymatic probing of $tRNA^{Lys3}$ with ribonuclease V1. The 3′ end labelled $tRNA^{Lys3}$, ([α-^{32}P]pCptRNA^{Lys3}), free or complexed with the U5-PBS region of viral RNA (nucleotides 1–545) was incubated for 7 min at 37°C in the presence of 0, 0.001, 0.005 and 0.01 U RNase (lanes 2–5 and 6–9, respectively). Lane 1 corresponds to untreated labelled $tRNA^{Lys3}$ and lane M to the alkaline hydrolysis of $tRNA^{Lys3}$ (size ladder). (**B**) Enzymatic probing with the MBN. Free 5′ end labelled $tRNA^{Lys3}$ or complexed with viral RNA was incubated for 7 min at 37°C in the presence of 0, 0.01, 0.05 and 0.1 U enzyme (lanes 2–5 and 6–9, respectively). Lane 1 corresponds to untreated labelled $tRNA^{Lys3}$. (**C**) Schematic representation of reactivity to nucleases of free $tRNA^{Lys3}$ or hybridised to HIV-2_{ROD} PBS. The black dots represent MBN cleavages, and the grey triangles represent the sites of cleavage by ribonuclease V1. The preferential cleavage sites of each nuclease are indicated by the increasing number of symbols depicted beside the nucleotides.

lane 7, and lane 4 with lane 8) after tRNA annealing to vRNA. In addition, new weak bands appeared, corresponding to digestion at positions A_{23}, G_{24}, Ψ_{27} and C_{40}.

After treatment with MBN (Fig. 2B), practically no differences appeared in the digestion patterns of tRNA either alone or complexed to RNA, indicating that the stem–loop structure of the anticodon and the D-loop domains were maintained within the primer–template complex. Interestingly, while the bands obtained by MBN digestion were more intense in the presence of viral RNA, especially for nucleotides D_{47}, A_{38} and R_{37}, the reactivity of the nucleotide U_{36} seemed to be lower (Fig. 2B).

From these results it may be concluded that upon formation of the initiation complex, the region $_{48}m^5Cm^5CAG_{51}$ of the TΨC loop must be engaged in a double-stranded secondary structure. Similarly, the relative protection of U_{36} in the anticodon loop could be due to its internal position within the complex. However, the increase in reactivity of nucleotides R_{37} and A_{38} does not favour this hypothesis. The anticodon could also be engaged in a double-stranded structure. Thus, these two regions could be in interaction with other domains of the viral RNA.

Probing of the U5 region from HIV-2_{ROD} RNA

HIV-2 RNA was probed using the same nucleases and experimental conditions described above. In this case, however, the enzymatic cleavages within RNA were identified by using primer extension assays. Reverse transcription of the resulting prePBS fragments was performed with an anti-PBS ODN primer. The synthesis bands were visualised by radioactive labelling (see Materials and Methods). The full cDNA synthesis product before nuclease treatment is shown in Figure 3A (lane C). The intermediate bands correspond to pausing sites of reverse transcription. After nuclease treatment the cleavage sites were defined either by the appearance of new radioactive bands, or by an increase in the already existing ones.

Digestion of the prePBS region (nucleotides 244–305). The results of viral RNA digestion in the absence of $tRNA^{Lys3}$ are presented and summarised in Figure 3. Treatment of viral RNA with MBN revealed highly accessible regions such as the triplets $_{279}GAG_{281}$ and $_{287}AAA_{289}$ and the nucleotides G_{285} and C_{294} (Fig. 3A, lanes 1–3). Although MBN is specific to single-stranded regions, the majority of the cleavage sites corresponded to nucleotides involved in a double-stranded region, according to the secondary structure model proposed by

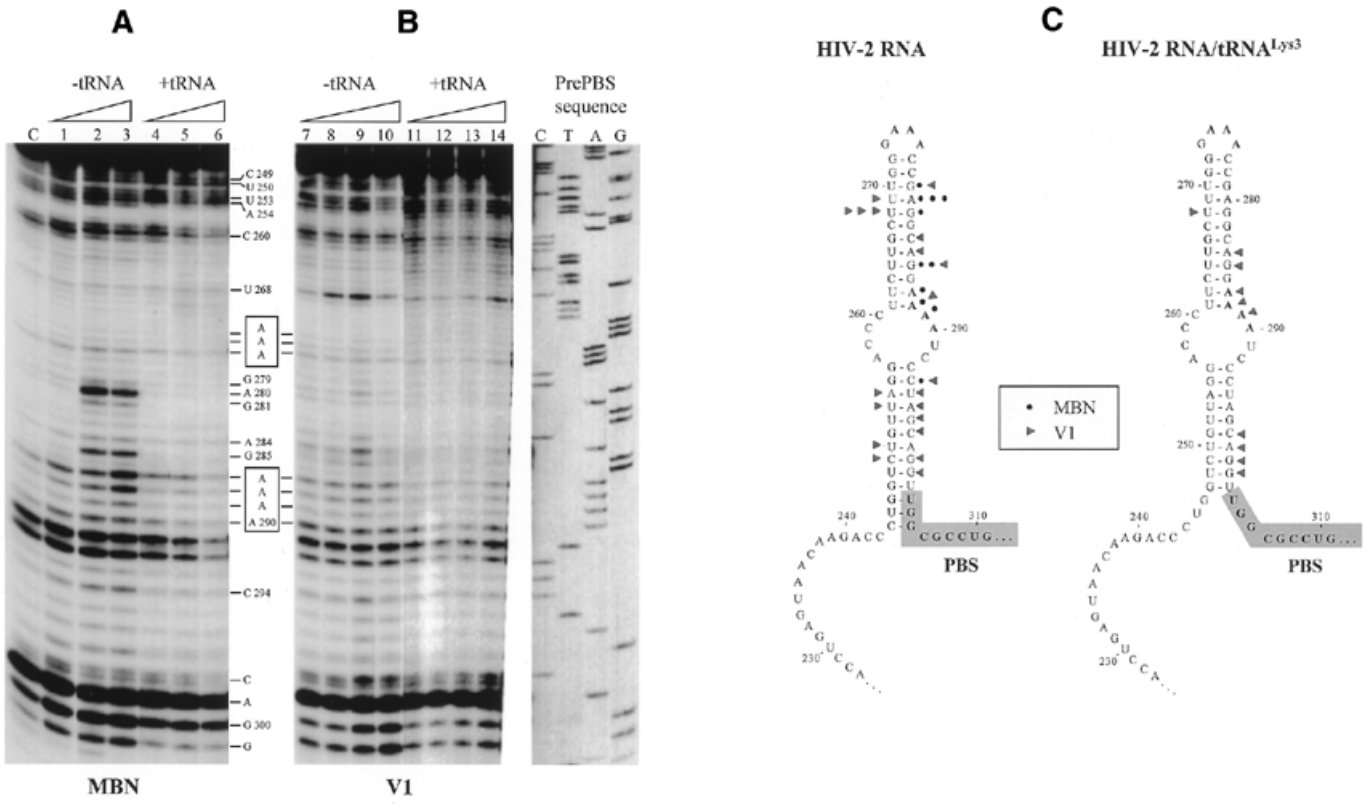

Figure 3. Digestion patterns of the HIV-2_{ROD} viral RNA complexed or not with $tRNA^{Lys3}$. The cleavage sites were detected by reverse transcription of the digested fragments by using an anti-PBS ODN primer. (**A**) Enzymatic digestion of the prePBS RNA (nucleotides 244–305) with MBN. The viral RNA complexed or not with $tRNA^{Lys3}$ was incubated for 7 min at 37°C in the presence of 0, 0.05 and 0.1 U enzyme (lanes 1–3 and 4–6, respectively). Lane C corresponds to the reverse transcription products on the viral RNA fragment before any nuclease treatment. (**B**) Viral RNA reactivity to ribonuclease V1. Free viral RNA or complexed to $tRNA^{Lys3}$ was incubated for 7 min at 37°C in the presence of 0, 0.001, 0.005 and 0.01 U enzyme (lanes 7–10 and 11–14, respectively). The prePBS sequence was used as a size marker. (**C**) Schematic representation of the prePBS-PBS HIV-2_{ROD} RNA region hybridised or not to the $tRNA^{Lys3}$. Reactivities to nucleases. The black dots correspond to sites of cleavage by MBN, and the grey triangles to those by ribonuclease V1. The preferential cleavage sites of each nuclease are indicated by the increasing number of symbols depicted beside the nucleotides.

Berkhout and Schoneveld (13). These authors also observed a sensitivity of certain double-stranded regions (including A_{280}, A_{287} and A_{288}) to dimethyl sulfate, diethyl pyrocarbonate and ribonuclease T1, which are normally specific agents of single-stranded molecules.

When the digestion was performed in the presence of RNase VI, cleavages were distributed throughout the prePBS region (Fig. 3B, lanes 7–10). Some cleavage sites coincided with those obtained with MBN. These results may be due to the fact that the U5 region of viral RNA (Fig. 3C), and more specifically the apical stem–loop (nucleotides 261–288), is a dynamic structure that can be transitorily destabilised. This is in agreement with the secondary structure of the 244–305 region described previously (13).

Digestion of the prePBS-PBS RNA region annealed to primer $tRNA^{Lys3}$. After annealing the viral RNA to tRNA, the binary complex was digested by MBN (Fig. 3A, lanes 4–6). Upon complex formation we observed a decreased sensitivity of all nucleotides that were reactive towards MBN in the free viral RNA, thus showing a protection of viral RNA by $tRNA^{Lys3}$.

Similarly, the presence of $tRNA^{Lys3}$ on the PBS protected the prePBS region from ribonuclease V1 attack (Fig. 3B, lanes 11–14). However, at the highest concentration of V1 used, weak but significant cleavage bands appeared as with the free template. This was the case with nucleotides U_{268}, A_{284} and G_{285}, thus indicating that the apical stem–loop structure is maintained. It was also the case for nucleotides C_{298}, A_{299}, G_{300} and G_{301}, showing that the stem–loop structure adjacent to the PBS was also conserved.

Mutated viral RNAs

To substantiate our results regarding the eventual interaction between the U-rich anticodon loop of $tRNA^{Lys3}$ and one of the two A-rich loops of the HIV-2 U5 region, we combined site-directed mutagenesis and probing with MBN. The two A-rich regions of the HIV-2 RNA prePBS region (stem–loop comprising nucleotides 244–305) were mutated independently (Fig. 4). Two fragments with different sequences in the A-rich regions were constructed: a $mut_{(274–276)}$ RNA with a CUU instead of the wild-type triplet $_{274}AAA_{276}$ on the apical loop, and a $mut_{(287–290)}$ RNA with an AGUU instead of $_{287}AAAA_{290}$ on the internal loop. The thermodynamic stability of each mutated RNA was then calculated and compared to that of wild-type RNA. Although the values obtained were similar for the three RNAs (Fig. 4) the substitution of the A nucleotides

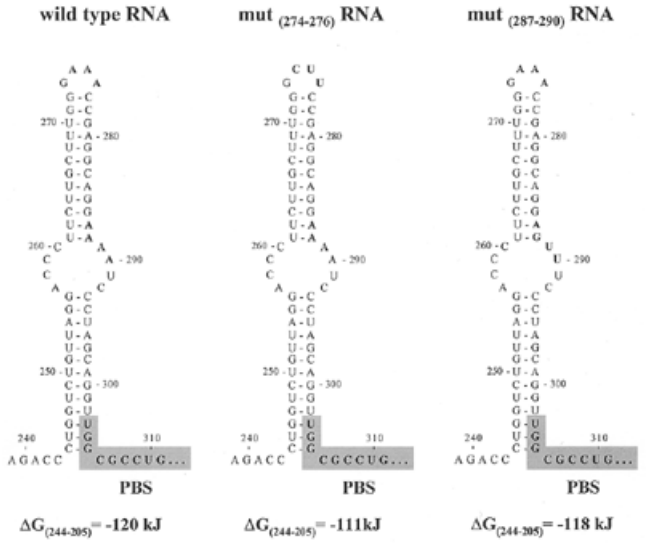

Figure 4. Stem–loop structures of the HIV-2_{ROD} RNA prePBS region. The prePBS region corresponding either to wild-type RNA, $mut_{(274–276)}$ RNA or $mut_{(287–290)}$ RNA is represented. The stability values corresponding to the three structures presented in this figure were determined by using the Zuker program.

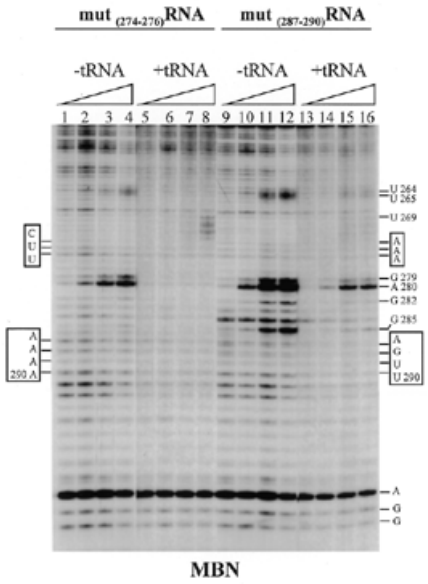

Figure 5. MBN digestion patterns of the mutated HIV-2^{ROD} viral RNAs complexed or not with $tRNA^{Lys3}$. Conditions were the same as those described in Figure 3. The $mut_{(274–276)}$ and $mut_{(287–290)}$ RNA fragments were incubated for 7 min at 37°C in the presence of 0, 0.001, 0.05 and 0.1 U enzyme, in the absence of $tRNA^{Lys3}$ (lanes 1–4 and 9–12, respectively) or hybridised to the $tRNA^{Lys3}$ (lanes 5–8 and 13–16, respectively).

led to a small decrease in the stability of the stem–loop, especially for $mut_{(274–276)}$ RNA. Both mutants were then tested for their sensitivity towards MBN in the absence or in the presence of $tRNA^{Lys3}$.

Digestion of mutated RNA in the absence of $tRNA^{Lys3}$. Although the MBN digestion patterns of $mut_{(274–276)}$ RNA and $mut_{(287–290)}$ RNA were rather similar (Fig. 5), some differences in sensitivity of mutated RNAs were observed. For example, in $mut_{(287–290)}$ RNA, nucleotides U_{264} and U_{265} were more accessible than in the wild-type or in the $mut_{(274–276)}$ RNA. This is probably due to differences in the stability of the stem–loop caused by changes in the sequence, thereby making some regions of the RNA more accessible.

Digestion of mutated RNAs in the presence of $tRNA^{Lys3}$. Like wild-type, $mut_{(274–276)}$ RNA became resistant to the attack by MBN in the presence of $tRNA^{Lys3}$ (Fig. 5, lanes 5–8). The new cleavage sites (U_{269}, U_{270}, G_{271} and G_{272}) at the highest nuclease concentration used can be explained by the decrease in stability of the prePBS stem–loop (ΔG = –111 kJ). The second mutated RNA, $mut_{(287–290)}$, also showed increased resistance to nuclease digestion in the presence of $tRNA^{Lys3}$. However, contrary to wild-type and $mut_{(274–276)}$ RNA, important cleavage fragments were still observed at position A_{280}, and to a lesser extent at A_{279}, G_{282} and G_{285}.

Thus, two different situations were observed in the presence of the natural primer $tRNA^{Lys3}$: (i) wild-type and $mut_{(274–276)}$ RNA were completely protected by $tRNA^{Lys3}$ against digestion by MBN and (ii) the $mut_{(287–290)}$ RNA was only partially protected by $tRNA^{Lys3}$. This partial protection implies that even if the $tRNA^{Lys3}$ is annealed to the PBS of this mutated RNA, the stability of the initiation complex is significantly modified.

The reactivity of the prePBS region towards MBN and ribonuclease V1 does not allow the direct observation of a possible interaction between the anticodon loop of the natural primer and one of the two A-rich loops of the HIV-2 RNA. However, the comparison of the digestion patterns obtained with the wild-type and the mutated RNAs strongly supports the interaction between the $tRNA^{Lys3}$ anticodon and the internal A-rich loop within the initiation complex.

Study of the (321–371) region from viral RNA

To determine whether the region 321–371 at the 3′ end of the PBS involved in a stem–loop interaction with the U5 region (Fig. 1) was implicated in the initiation complex, we used the same protocol described above (Fig. 3). This time the cleavage sites were identified by reverse transcription from a hybridised primer in the region 372–390. Figure 6A shows the MBN digestion pattern of the RNA region comprising nucleotides 321–371, either free or in the duplex with tRNA (lanes 1–3 and 4–6, respectively). Data are summarised in Figure 6B.

The two digestion profiles were identical in the presence or absence of $tRNA^{Lys3}$. The main cleavage sites A_{368} and G_{335} corresponded to the two loops in the secondary structure model. It may be concluded that there is no modification of the secondary structure of the fragment 206–226/321–371 upon formation of the template–primer complex, thus showing that the 321–371 region is not involved in an interaction with $tRNA^{Lys3}$.

A secondary structure model of the HIV-2 $tRNA^{Lys3}$–RNA complex

As described above we used structure-specific nucleases to map both viral RNA and tRNA primer secondary structures before and after formation of the HIV-2 RNA–tRNA

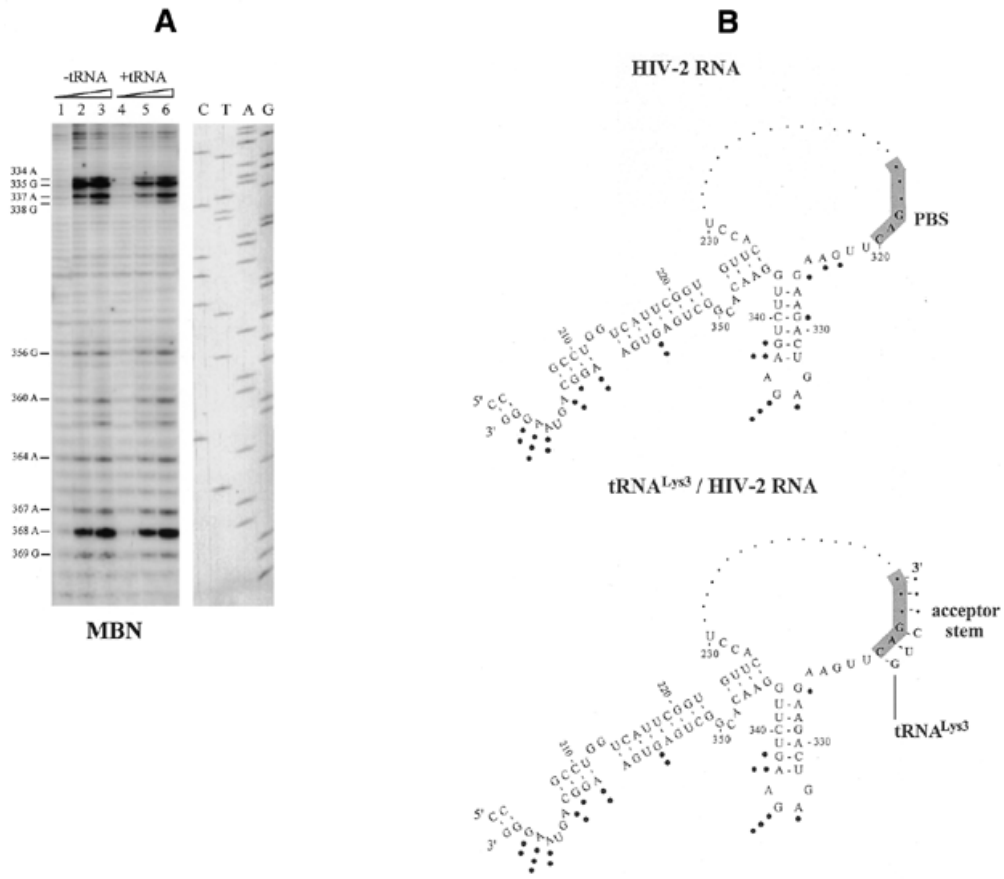

Figure 6. (**A**) MBN digestion patterns of the HIV-2_{ROD} RNA (321–371) region complexed or not with the natural tRNA^{Lys3} primer. The cleavage sites were evidenced by reverse transcription of the digested products from wild-type RNA using an ODN primer complementary to nucleotides 372–390. The viral RNA complexed or not with the tRNA^{Lys3} was incubated for 7 min at 37°C in the presence of 0, 0.05 and 0.1 U enzyme (lanes 1–3 and 4–6, respectively). The sequence of the RNA fragment was used as size marker. (**B**) Schematic representation of reactivity to MBN of the HIV-2_{ROD} RNA region (nucleotides 321–371) complexed or not to tRNA^{Lys3}. The MBN cleavage sites are indicated by black dots, and the level of viral RNA sensitivity by the number of symbols.

template–primer complex. Upon complex formation, the $_{287}$AAAA$_{290}$ region of the U5-prePBS internal loop was protected, thus showing an interaction with tRNA (Figs 3 and 5). Moreover, the $_{48}$m^{5}Cm^{5}CAG$_{51}$ region was highly degraded by ribonuclease V1 when tRNA was annealed to the PBS (Fig. 2), thereby pointing to the existence of a double-stranded region between nucleotides 48 and 51 of tRNA^{Lys3} and a complementary sequence of the viral RNA.

The analysis of the U5 domain showed a sequence presenting a perfect match with the region 48–55 of the TΨC stem–loop. In view of these observations, an interaction may be predicted between the region 240–247 of HIV-2 RNA and the complementary region (nucleotides 48–55) of the TΨC domain upon formation of the initiation complex. In relation to this, it is important to point out that when Berkhout and Schoneveld proposed their structural model of HIV-2 RNA, they already raised the possibility of having a base-paired region between the TΨC loop of tRNA^{Lys3} and this 5′ region upstream of the PBS (13).

To further assess the biological importance of the interactions with U5, we analysed the sequences of this region from 16 HIV-2 isolates (Table 1). We considered only the isolates that have been completely sequenced and are available in Internet databases. From this analysis we can conclude the following. (i) The changes affecting the whole prePBS stem–loop (positions 244–305) are essentially distributed within the apical stem–loop (nucleotides 261–298). In fact, 13 isolates out of 16 presented at least one mutation in this hairpin. In contrast, only five isolates out of 16 showed the same change within the stem 244–256/293–305, in which the nucleotide G_{301} is replaced by an A. However, most of the changes altering the double strand did not lead to a modification of the RNA secondary structure, because they corresponded to compensatory mutations, e.g., the formation of U-A or C-G base pairs instead of U-G. This is in agreement with previous phylogenetic and mutagenesis data obtained from HIV-1 (18,19). It was suggested that mutations modifying the stability of the prePBS hairpin were able to disturb both tRNA annealing and initiation of reverse transcription. In HIV-2, the lower stem of prePBS seems to play a similar role. (ii) In six isolates out of 16, the $_{274}$AAA$_{276}$ triplet is replaced by GAA or AAU, while the sequence $_{287}$AAAA$_{290}$ is perfectly conserved. This observation underlines the importance of this region in the formation of the initiation complex. (iii) Similarly, five changes were found in the 230–250 region, (G_{231}, A_{232}, G_{233}, A_{235} and A_{236}), while no changes for nucleotides involved in

Table 1. Sequence alignment of the prePBS-PBS region of different subtypes of HIV-2 isolates

ISOLATE	SUBTYPE	240-247 REGION	APICAL A-RICH LOOP	INTERNAL A-RICH LOOP	PBS REGION
ROD	A	GUUCACCUGAGUAACAAGACCCUGGUCUGUUAGGACCCUUCUUGCUUUGGGAAACCGAGGCAGGAAAAUCCCUAGCAGGUUGGCGCCUGAACAGGGAC			
YSY	A	GUUCUCCUGAGUAACAAGACCCUGGUCUGUUAGGACCCUUCUUGCUUUGGGAAACCGAGGCAGGAAAAUCCCUAGCAGGUUGGCGCCCGAACAGGGAC			
MDS	A	GUUCACCUGAAUAACAAGACCCUGGUCUGUUAGGACCCUUCUUGCUUUGGGAAACCGAGGCAGGAAAAUCCCUAGCAGGUUGGCGCCCGAACAGGGAC			
CAM2CG	A	GUUCACCUGAAUAACAAGACCCUGGUCUGUUAGGACCCUUCUUGCUUUGGGAAACCAAGGCAGGAAAAUCCCUAGCAGGUUGGCGCCCGAACAGGGAC			
ALI	A	GUUCACCUGAGUAACAAGACCCUGGUCUGUUAGGACCCUUUCUGCUUUGGGAAACGGAGGCAGGAAAAUCCCUAGCAGGUUGGCGCCCGAACAGGGAC			
BEN	A	GUUCAUCUGAGUAACAAGACCCUGGUCUGUUAGGACCCUUCUCGCUUUGGGAAUCCAAGGCAGGAAAAUCCCUAGCAGGUUGGCGCCCGAACAGGGAC			
D194	A	GUUCAUCUGAGUAACAAGACCCUGGUCUGUUAGGACCCUUCCCGCUUUGAGAAUCCAAGGCAGGAAAAUCCCUAGCAGGUUGGCGCCCGAACAGGGAC			
UC2	A	GUUCAUCUGAGUAACAAGACCCUGGUCUGUUAGGACCCUUCCCGCUUUGGGAAUCCAAGCGGGAAAAUCCCUAGCAGGUUGGCGCCCGAACAGGGAC			
HIV2ST	A	----------AGUAACAAGACCCUGGUCUGUUAGGACCCUUUCUGCUUUGGGAAACCAAGGCAGGAAAAUCCCUAGCAGGUUGGCGCCCGAACAGGGAC			
PEI2	A	GUUCACCUAAGUGACAAGACCCUGGUCUGUUAGGACCCUUCUUGCUUUGGGGAACCGAAGCGGGAAAAUACCUAGCAGAUUGGCGCCCGAACAGG---			
GH1	A	GUUCAUCUGAAUAACAAGACCCUGGUCUGUUAGGACCCUUCC-GCUUUGGGAAUCCAAGGCAGGAAAAUCCCUAGCAGGUUGGCGCC-GAACAGGGAC			
FG	A	GUUCACCUGUAUAACAAGACCCUGGUCUGUUAGGACCCUUCUUGCUUUGGGAAACCGAGGCAGGAAAAUCCCUAGCAGGUUGGCGCCCGAACAGG---			
D205 ALT	B	----------------AGACCCUGGUCUGUUAGGACCCUUCUUGCUUUGGGAAACCGAAGCGGGAAAAUCCCUAGCAGAUUGGCGCCCGAACAGGGAC			
UC1	B	----------------AAGACCCUGGUCUGUUAGGACCCUUUCUGCUUUGGGAAACCAAGGCAGGAAAAUCCCUAGCAGAUUGGCGCCCGAACAGGGAC			
EHO	B	------------------ACCCUGGUCUGUUAGGACCCCUUCUGCUUUGGGAAACCAAGGCAGGAAAAUCCCUAGCAGAUUGGCGCCCGAACAGGGAC			
ABT96	G	GUUCGC----GUAGCAAGACCCUGGUCUGUUAGGACCCUUUCUGCUUUGGRGAACCAGAGCGGGAAAAUCCCUAGCAGAUUGGCGCCCGAACAGGGAC			

the interaction of viral RNA with the TΨC stem–loop were observed.

Since the HIV-2 RNA ROD isolate has a U instead of a C at position 310 within the PBS, some authors have raised the possibility that an alternative primer, $tRNA^{Lys5}$ (also called $tRNA^{Lys7}$), may be used (20,21). This variant differs from $tRNA^{Lys3}$ at five nucleotide positions. Interestingly, the change m^5C_{48}-U was found, which is involved in the interaction with viral RNA. This change leads to the formation of a base pair G_{247}/U_{48} instead of G_{247}/m^5C_{48} that should not influence the structure of the HIV-2 initiation complex established in this work.

By using enzymatic probing data and sequence comparison, we propose a structural model of the HIV-2 primer–template reverse transcription initiation complex (Fig. 7). This model comprises the secondary structure elements in interaction: (i) the viral PBS and the 3′ end acceptor stem of $tRNA^{Lys3}$ that serves as *stricto sensu* primer; (ii) the U-rich region of the anticodon loop and the A-rich sequence of the internal loop ($_{287}AAAA_{290}$) contained in the prePBS region; (iii) nucleotides 48–54 from the TΨC domain of tRNA with the region 240–247 of viral RNA.

This HIV-2 model is similar to that described for HIV-1 (4), mainly concerning the interaction between the U-rich sequence of the anticodon and the A-rich sequence of the viral prePBS. However, there are some significant differences. In contrast to HIV-1, no intramolecular changes were observed in the structure of the HIV-2 binary complex. In this sense, the HIV-2 complex is similar to that described for Rous sarcoma virus (RSV) (22), where only the TΨC domain of $tRNA^{Trp}$ interacts with the U5 RNA.

The use of site-directed mutagenesis and nuclease footprinting approaches allowed us to define the secondary structure of two crucial RNA partners of the HIV-2 initiation complex. These results should help to overcome the absence of appropriate crystals allowing the study of the 3D structure of this complex. Furthermore, the interactions inferred from these studies are in good agreement with the kinetic results we reported previously for the *in vitro* study of HIV-2 reverse transcription (23). As in the case of HIV-1 and RSV (24,25), tRNA primed cDNA synthesis in HIV-2 occurs in two steps: a slow and distributive initiation step, and a fast and processive elongation process. From these results obtained with these three retroviruses, it can be proposed a unifying model of the initiation of reverse transcription, which links the primer–template interactions with the emergence of the two kinetic steps mentioned above. However, although HIV-1, RSV and HIV-2 seem to have a similar mechanism for the initiation of

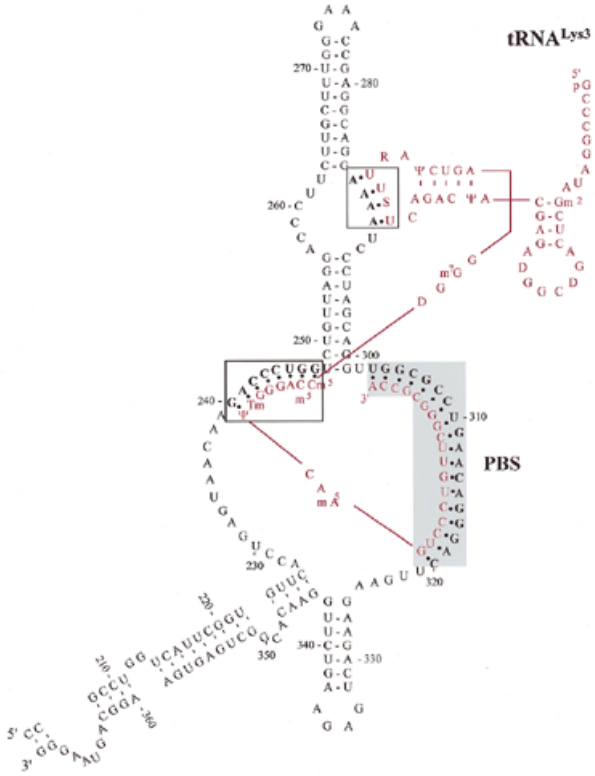

Figure 7. Structural model of the HIV-2_{ROD}–$tRNA^{Lys3}$ binary complex. The shaded box corresponds to the principal interaction PBS–acceptor stem. The white boxes correspond to the additional interactions: A-rich sequence of the internal loop with the U-rich loop of the anticodon; nucleotides 48–54 from the TΨC domain of tRNA with the region 240–247 of viral RNA.

cDNA synthesis, they present different secondary structures of the initiation primer–template duplex.

Further work is necessary to ascertain the structure–function relationship of the nucleic acids and protein partners of the retroviral initiation complex. This approach will help to fully understand the mechanism of reverse transcription and to design new inhibitors able to interfere with the structure of the initiation complex, a critical target in the fight against HIV infection.

ACKNOWLEDGEMENTS

This work was supported in part by the Centre National de la Recherche Scientifique (CNRS), the Université Victor Segalen Bordeaux 2, the Agence Nationale de Recherches contre le SIDA (ANRS) and the Pôle Médicament (Conseil Régional d'Aquitaine).

REFERENCES

1. Telesnitsky,A. and Goff,S.P. (1997) Reverse transcriptase and the generation of retroviral DNA. In Coffin,J.M., Hughes,S.H. and Varmus,H.E. (eds), *Retroviruses*. Cold Spring Laboratory Press, Cold Spring Harbor, NY, pp. 121–160.
2. Arts,E.J. and Le Grice,S. (1998) Interaction of retroviral reverse transcriptase with template–primer duplexes during replication. *Prog. Nucleic Acids Res. Mol. Biol.*, **58**, 335–394.
3. Isel,C., Marquet,R., Keith,G., Ehresmann,C. and Ehresmann,B. (1993) Modified nucleotides of $tRNA^{Lys3}$ modulate primer/template loop–loop interaction in the initiation complex of HIV-1 reverse transcription. *J. Biol. Chem.*, **268**, 25269–25272.
4. Isel,C., Ehresmann,C., Keith,G., Ehresmann,B. and Marquet,R. (1995) Initiation of reverse transcription of HIV-1: secondary structure of the HIV-1 RNA/$tRNA^{Lys3}$ (template/primer). *J. Mol. Biol.*, **247**, 236–250.
5. Skripkin,E., Isel,C., Marquet,R., Ehresmann,B. and Ehresmann,C. (1996) Psoralen crosslinking between HIV-1 RNA and primer $tRNA^{Lys3}$. *Nucleic Acids Res.* **24**, 509–514.
6. Wakefield,J.K., Rhim,H. and Morrow,C.D. (1994) Minimal sequence requirements of a functional HIV-1 primer binding site. *J. Virol.*, **68**, 1605–1614.
7. Huang,Y., Shalom,A., Li,Z., Wang,J., Mak,J., Wainberg,M.A. and Kleiman,L. (1996) Effects of modifying the $tRNA^{Lys3}$ anticodon on the initiation of HIV-1 reverse transcription. *J. Virol.*, **70**, 4700–4706.
8. Liang,C., Li,X., Rong,L., Inouye,P., Quan,Y., Kleiman,L. and Wainberg,M.A. (1997). The importance of the A-rich loop in HIV-1 reverse transcription and infectivity. *J. Virol.*, **71**, 5750–5757.
9. Kang,S.M., Zhang,Z. and Morrow,C.D.(1997) Identification of a sequence within U5 required for HIV-1 to stably maintain a primer binding site complementary to $tRNA^{Met}$. *J. Virol.*, **71**, 207–217.
10. Wakefield,J.K., Kang,S.M. and Morrow,C.D. (1996) Construction of a type-1 HIV that maintains a primer binding site complementary to $tRNA^{His}$. *J. Virol.*, **70**, 966–975.
11. Zhang,Z., Kang,S.M., LeBlanc,A., Hajduk,S.L. and Morrow,C.D. (1996) Nucleotide sequences within the U5 region of the viral RNA genome are the major determinants for an HIV-1 to maintain a primer binding site complementary to $tRNA^{His}$. *Virology*, **226**, 306–317.
12. Li,Y., Zhang,Z., Wakefield,J.K. and Morrow,C.D. (1997) Nucleotide substitutions within U5 are critical for efficient reverse transcription of HIV-1 with a primer binding site complementary to $tRNA^{His}$. *J. Virol.*, **71**, 6315–6322.
13. Berkhout,B. and Schoneveld,I. (1993) Secondary structure of the HIV-2 leader RNA comprising the tRNA-primer binding site. *Nucleic Acids Res.*, **21**, 1171–1178.
14. Zuker,M. (2000) Calculating nucleic acid secondary structure. *Curr. Opin. Struct. Biol.*, **10**, 303–310.
15. Boulmé,F., Freund,F., Gryaznov,S., Nielsen,P.E., Tarrago-Litvak,L. and Litvak,S. (2000) Study of HIV-2 primer-template initiation complex using antisense oligonucleotides. *Eur. J. Biochem.*, **267**, 2803–2811.
16. Sallafranque-Andreola,M.L., Robert,D., Barr,P.J., Fournier,M., Litvak,S., Sarih-Cottin,L. and Tarrago-Litvak,L. (1989) HIV reverse transcriptase expressed in transformed yeast cells. Biochemical properties and interaction with $tRNA^{Lys3}$. *Eur. J. Biochem.*, **184**, 367–374.
17. Boulmé,F., Freund,F., Moreau,S., Nielsen,P.E., Gryaznov,S., Toulmé,J.J. and Litvak,S. (1998) Modified (PNA, 2′-*O*-methyl and phosphoramidate) anti-TAR antisense oligonucleotides as strong and specific inhibitors of *in vitro* HIV-1 reverse transcription. *Nucleic Acids Res.*, **26**, 5492–5500.
18. Berkhout,B. (1997) The primer binding site on the RNA genome of human and simian immunodeficiency viruses is flanked by an upstream hairpin structure. *Nucleic Acids Res.*, **25**, 4013–4017.
19. Beerens,N., Groot,F. and Berkhout,B. (2000) Stabilization of the U5-leader stem in the HIV-1 RNA genome affects initiation and elongation of reverse transcription. *Nucleic Acids Res.*, **28**, 4130–4137.
20. Lauerman,V., Peden,K. and Boeke,J.D. (1996) Alternative tRNA primers for HIV. *AIDS*, **10**, 1738–1740.
21. Das,A.T., Klaver,B. and Berkhout,B. (1997) Sequence variation of the HIV primer binding site suggests the use of an alternative $tRNA^{Lys}$ molecule in reverse transcription. *J. Gen. Virol.*, **78**, 837–840.
22. Morris,S. and Leis,J. (1999) Changes in Rous sarcoma virus RNA secondary structure near the primer binding site upon $tRNA^{Trp}$ primer annealing. *J. Virol.*, **73**, 6307–6318.
23. Boulmé,F., Freund,F. and Litvak,S. (1998) Initiation of *in vitro* reverse transcription from $tRNA^{Lys3}$ on HIV-1 and HIV-2 RNAs by both type 1 and type-2 reverse transcriptases. *FEBS Lett.*, **430**, 165–170.
24. Lanchy,J.M., Ehresmann,C., Le Grice,S., Ehresmann,B. and Marquet,R. (1996) Binding and kinetic properties of HIV-1 reverse transcriptase markedly differ during initiation and elongation of reverse transcription. *EMBO J.*, **15**, 7178–7187.
25. Isel,C., Ehresmann,C., Keith,G., Ehresmann,B. and Marquet,R. (1997) Two step synthesis of (–) strong-stop DNA by avian and murine reverse transcriptases *in vitro*. *Nucleic Acids Res.*, **25**, 545–552.